Journal of Thermal Science and Technology

[Review Paper]

Recent advances in strategies for inhibiting Leidenfrost effect

Huaduo GU*, Mingyu LI**, Jiahao ZHANG*** and Zuankai WANG*,***

*Department of Mechanical Engineering, Hong Kong Polytechnic University 11 Yuk Choi Road, Kowloon, Hong Kong SAR, 999077, China E-mail: zk.wang@polyu.edu.hk

**Department of Mechanical Engineering, City University of Hong Kong 83 Tat Chee Avenue, Kowloon, Hong Kong SAR, 999077, China

***Shenzhen Research Institute of Hong Kong Polytechnic University

No. 18, Yuexing 1st Road, South District, High-tech Industrial Park, Yuehai Street, Nanshan District, Shenzhen, 518000, China

Received: 10 October 2024; Revised: 16 January 2025; Accepted: 28 February 2025

Abstract

The rapid progression of industrialization and the integration of artificial intelligence in recent years emphasizes the critical need for efficient thermal cooling solutions. Despite significant strides in technology, existing liquid cooling methods, notably boiling heat transfer and spray cooling, encounter substantial obstacles attributable to the well-documented Leidenfrost effect. Upon contact with a highly heated surface, a liquid generates a vapor layer that acts as an insulator, elevating the liquid above the surface and severely impeding heat transfer efficiency. While notable advancements have been achieved in mitigating the Leidenfrost effect, a comprehensive understanding of the underlying mechanisms remains limited. Furthermore, challenges persist in sustaining high-temperature environments across diverse structures, materials, and technologies, impeding progress in this domain. This review aims to provide a thorough account of fundamental tactics for suppressing the Leidenfrost phenomenon on high-temperature substrates. It will underscore distinctive attributes and challenges while exploring avenues for the development of efficient and sustainable thermal management solutions.

Keywords: Leidenfrost effect, Inhibition strategies, Extreme thermal management, Surface engineering, Liquid modification, External fields

1. Introduction

In the past decade, the swift advancement of industrialization and artificial intelligence, particularly in domains characterized by exceedingly high heat flux and elevated temperatures such as nuclear fusion cores (Tominaga et al., 2014), aerospace (Gu et al., 2023), data centers (Ebrahimi et al., 2014), and electronics (Van Erp et al., 2020), has precipitated an escalating demand for effective heat dissipation technologies. Under such circumences, the efficacy of liquid cooling methods, specifically boiling heat transfer and spray cooling, assumes paramount importance. Nonetheless, a persistent challenge encountered in phase-change liquid cooling on extremely hot surfaces is the Leidenfrost effect (Leidenfrost, 1756). As liquid approaches an ultra-hot surface, it immediately forms an insulating vapor layer, causing the liquid to suspend above the surface rather than making physical contact, as illustrated in Figs. 1(a-b). The vapor layer, characterized by substantial thermal resistance and high lubricity, predominantly obstructs the heat transfer between the substrate and the liquid. Additionally, the vapor coalescence on high-temperature surfaces may precipitate severe engineering accidents in heat transfer processes.

The onset of the Leidenfrost effect, known as the Leidenfrost point (LFP), signifies the initiation of stable film boiling. As depicted in Nakayama's boiling curve in Fig. 1(c), the LFP corresponds to the minimum heat flux (Berenson, 1962). Broadly, the LFP is contingent upon various factors, encompassing substrate morphology, droplet properties, and external fields. A higher Leidenfrost point typically indicates enhanced heat transfer capacity and reduced vulnerability to failures in liquid cooling, thus enhancing equipment stability and safety. In practical scenarios, such as spray cooling and fuel

injection, droplets often contact solid surfaces in the form of impact. When the impact velocity of the liquid is non-negligible, the minimum solid temperature at which the dynamic Leidenfrost effect manifests is referred to as the dynamic LFP (Shirota et al., 2016).

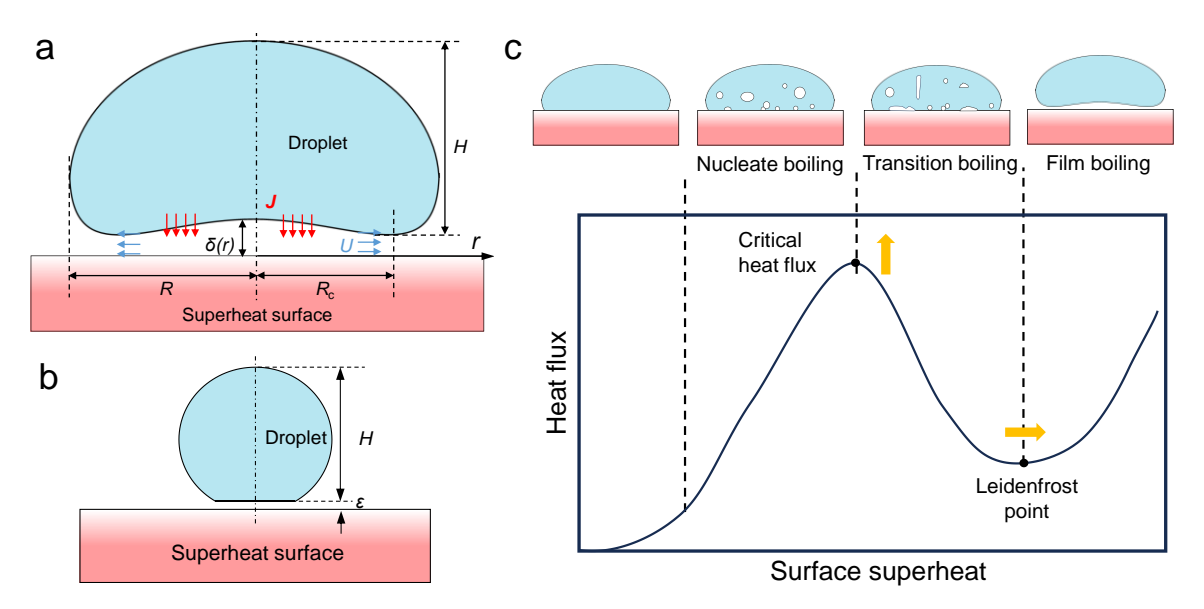


Fig. 1 Leidenfrost phenomenon. a) Quasi-spherical shape for the droplets with a radius $R < l_c$, and b) Pancake shape for the droplets with a radius $R \ge l_c$ (Biance et al., 2003; Quéré, 2013). c) Nakayama's boiling curve (Berenson, 1962).

The quest for strategies to suppress the Leidenfrost effect has emerged as a pivotal concern, drawing significant interest. Essentially, the manifestation of the Leidenfrost effect hinges on the interplay between liquid-solid contact and gas-solid contact. Over recent decades, a plethora of technologies aimed at mitigating the Leidenfrost effect has been explored by delaying or disrupting the formation of the vapor layer. These methods primarily involve surface functionalization (micro/nanopillars (Tran et al., 2013), porous materials (Nair et al., 2014; Sajadi et al., 2017), heterogeneous structures (Jiang et al., 2022)), fluid modifications (polymer additives (Bertola, 2009), surfactants (Prasad et al., 2022), and nanoparticles (Jollans and Orrit, 2019)), the and applications of external fields (acoustic field (Ng et al., 2016), mechanical vibration (Ng et al., 2015), electric field (Shahriari et al., 2017), pressure (Van Limbeek et al., 2021), gravity (Maquet et al., 2015)).

Despite the significant strides made in alleviating the Leidenfrost effect, several intriguing inquiries have emerged, such as how to further improve the Leidenfrost temperature, how to achieve the heat flux limit on high-temperature surfaces, and how to pinpoint the most cost-effective, straightforward-to-implement, and efficacious technology.

Based on the aforementioned concerns, we systematically summarize the strategies for suppressing the Leidenfrost effect, as presented in Fig. 2. Initially, we elucidate the foundational physical mechanisms, critical dynamics, and heat transfer principles linked to the Leidenfrost effect. Subsequently, we discuss various strategies to suppress the Leidenfrost effect, such as micro/nanoscale structures, fluid modifications, and external conditions, as well as the primary findings and underlying mechanisms. Lastly, we briefly explore the promising breakthroughs related to suppressing the Leidenfrost effect. This review not only summarizes the existing findings but also expects to inspire novel designs and advancements in tailored engineering surfaces for suppressing the Leidenfrost effect.

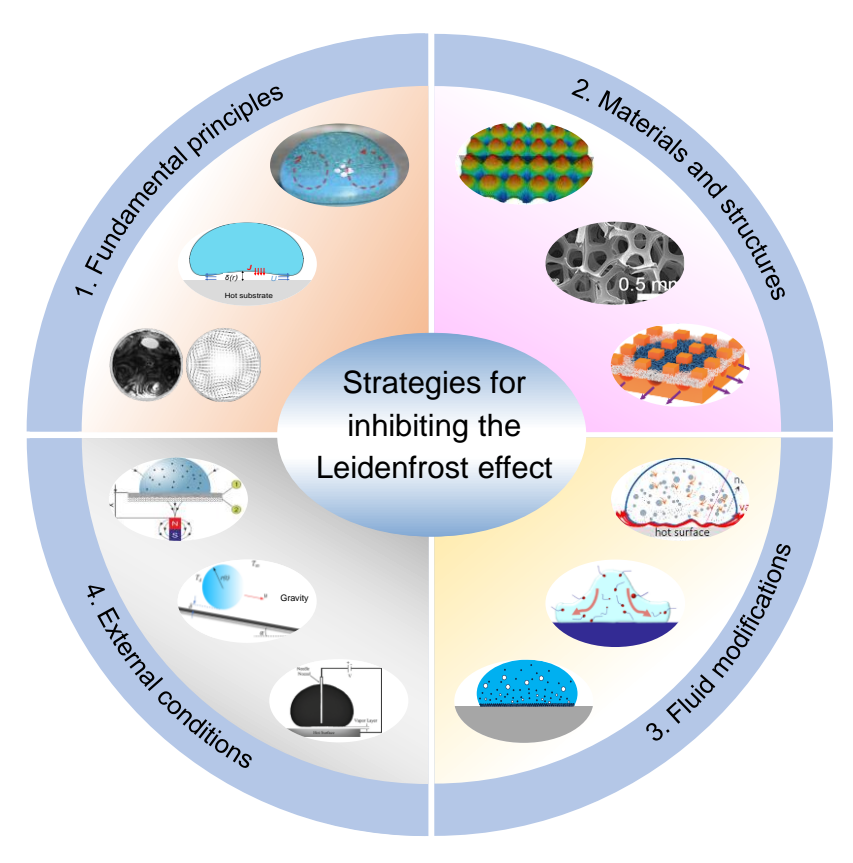


Fig. 2 Strategies for inhibiting the Leidenfrost effect.

2. Fundamental understanding

The Leidenfrost effect primarily arises from the competition between the liquid-vapor interactions and the vaporsolid interactions. Following this understanding, to better inhibit the Leidenfrost effect and improve the heat transfer efficiency of high-temperature surfaces, it becomes essential to elucidate the underlying hydrodynamics and thermodynamics of Leidenfrost droplets and vapor layers.

2.1 Droplet behaviors

The Leidenfrost droplet levitated on a vapor layer above a heated surface showcases either a quasi-spherical or pancake shape (Biance et al., 2003; Quéré, 2013), as displayed in Fig. 1. The capillary length of the liquid is defined as $l_c = \sqrt{\gamma/\rho_1 g}$, where γ , ρ_1 and g denote the surface tension, liquid density, and gravity acceleration. When the droplet radius R is smaller than the capillary length of the liquid, due to the balance between surface tension and hydrostatic pressure, the droplet presents a spherical shape, with an approximately flat bottom, a height of H = 2R, a neck radius of $R_c = \sqrt{\frac{2}{3}}R^2/l_c$, and a lifetime scaling as $\tau \sim \frac{\rho_1 h_{1V}}{\lambda_1 \Delta T_s}R_0^2$ (Biance et al., 2003). Here, R_o , λ_1 , h_{1V} , and ΔT_s represent the initial radius of the droplet, the thermal conductivity and the latent heat of the liquid, and the superheat of the surface. During the droplet evaporation, the radius depending on time is expressed as $R = R_o(1 - t/\tau)^{1/2}$. As the radius approaches capillary length, the gravity effect becomes more significant, and the droplet that is levitated on a nonuniform vapor layer displays a pancake shape. According to the differential equation of Laplace pressure, the pancake droplet in an equilibrium state has a height of $H = 2l_c$, a neck radius of $R_c = \sqrt{\frac{2}{3}}R^{3/2}/l_c^{1/2}$, and a lifetime of $\tau = 2\left(\frac{4\rho_1 l_c h_{1V}}{\lambda \Delta T_s}\right)^{3/4}\left(\frac{3\eta_V}{\rho_V g}\right)^{1/4}R_0^{1/2}$ (Biance et al., 2003). Here, η_V is the vapor viscosity. As the Leidenfrost droplet evaporates, the vapor layer becomes thin over time, the droplet not only retracts but also sinks slowly, finally, the radius of the Leidenfrost droplet becomes $R = R_o(1 - t/\tau)^2$ (Biance et al., 2003). When the radius of the droplet further increases

to a critical size $\sim 4l_c$, the Leidenfrost droplet will be subjected to strong instability, forming a steam chimney underneath the droplet that will gradually burst through the center of the droplet (Snoeijer et al., 2009).

The behaviors of Leidenfrost droplets (encompassing levitation, rotation, star oscillation, bouncing, etc.) vary from surface temperatures, substrate characteristics, liquid properties as well as the morphology of vapor layers (Bouillant et al., 2018; Bourrianne et al., 2019; Graeber et al., 2021; Li et al., 2023; Lin et al., 2024; Liu and Tran, 2020; Paul et al., 2015; Yang et al., 2022). Typically, the liquid-vapor interface at the bottom of the droplet ehibits higher temperatures compared to the liquid-air interface at the apex, potentially triggering thermobuoyant currents and Marangoni flows within the Leidenfrost droplet. These dynamics can lead to heightened horizontal and vertical rotation (Chakraborty et al., 2022; Yim et al., 2022), as shown in Figs. 3(a) and (b). These self-propulsion and self-rotation phenomena can be intensified by rapid asymmetric internal flow and bottom tilt (Bouillant et al., 2018) on asymmetrically textured surfaces (Dupeux et al., 2013), temperature gradient surfaces (Sobac et al., 2017) and wettability gradient surfaces (Agapov et al., 2014; Chen et al., 2018b). Modulating the distribution and configuration of hydrophilic and hydrophobic regions via chemical or physical means can exert a significant influence on the dynamics of Leidenfrost droplets and the cooling efficacy of high-temperature surfaces (Li et al., 2023; Yang et al., 2022). These behaviors provide substantial potential for localized thermal management.

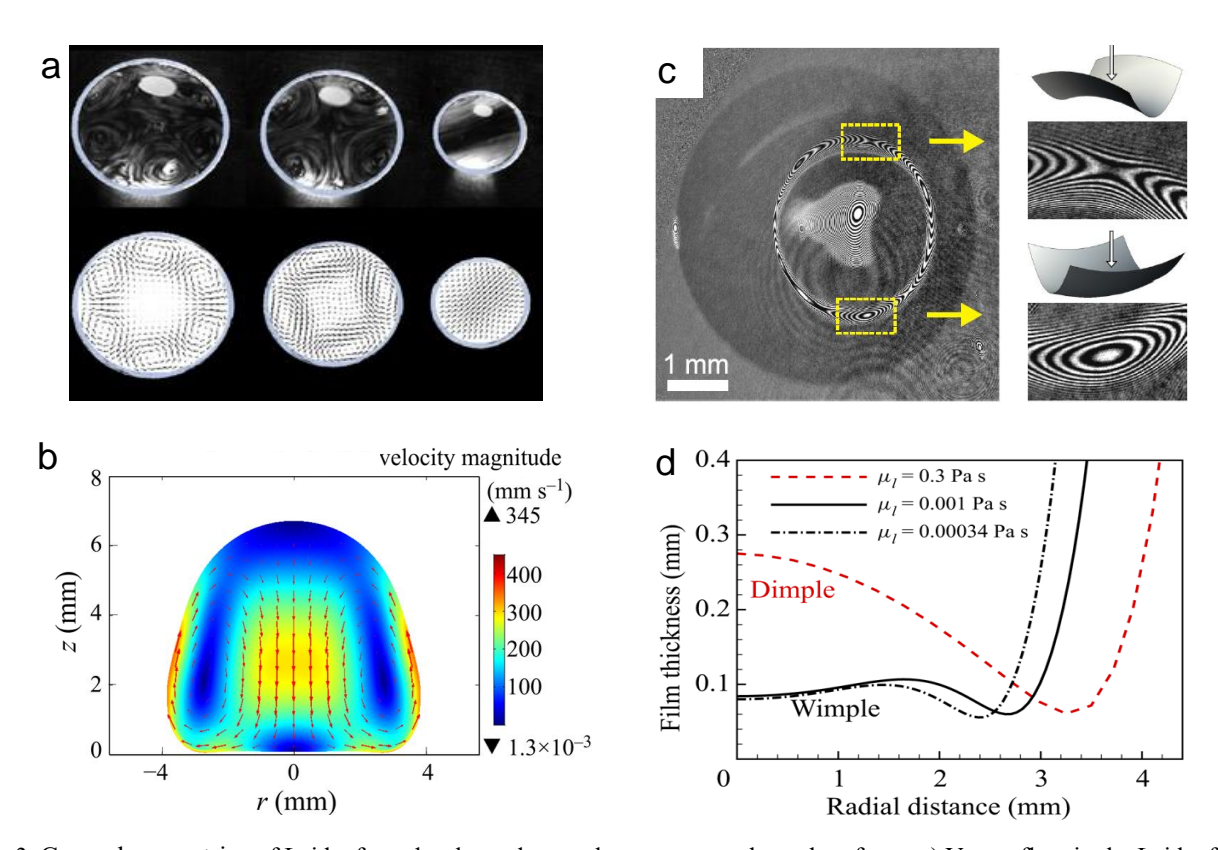


Fig. 3 General geometries of Leidenfrost droplet and vapor layers on superheated surfaces. c) Vortex flow in the Leidenfrost droplet (Yim et al., 2022). b) Velocity fields in the Leidenfrost droplet from simulations (Chakraborty et al., 2022). c) Interface images of the vapor film from experiments (Burton et al., 2012). d) The vapor film thickness from simulations (Chakraborty et al., 2022).

2.2 Vapor layer morphologies

The presence of the vapor layer is the primary factor contributing to the extended longevity of Leidenfrost droplets. Ensuring sufficient liquid-solid contact and efficient bubble detachment is imperative for sustaining elevated heat transfer efficiency. Hence, observing and disrupting vapor films within the Leidenfrost phenomenon has become an important focus for optimizing heat transfer efficiency on extremely high-temperature surfaces.

For the Leidenfrost droplets with a radius $R < l_c$, the vapor film is roughly flattened, with a thickness being derived as $\delta \sim \left(\frac{\lambda \Delta T_S \eta_V \rho_1 g}{h_{lv} \rho_v \gamma^2}\right)^{1/3} R^{4/3}$ (Biance et al., 2003). In contrast, for the Leidenfrost droplets with a radius $R \ge l_c$, the vapor

morphology is discovered to resemble the shape of an inverted bowl, allowing vapor to escape through Poiseuille flows. This leads to an average thickness of $\delta = \left(\frac{3\lambda_1\Delta T_8\eta_V}{4h_{1v}\rho_V\rho_1gl_c}\right)^{1/4}R^{1/2}$ (Biance et al., 2003). As the Leidenfrost droplet undergoes evaporation, the thickness of the vapor film decreases with time, which can be expressed mathematically as $\delta(t) = \left(\frac{3\lambda\Delta T_8\eta_VR_0^2}{4h_{1v}\rho_V\rho_1gl_c}\right)^{1/4}(1-t/\tau)$ (Biance et al., 2003). This relationship highlights the time-dependent nature of vapor film thickness as it responds to changing droplet dynamics during the evaporation process.

Extensive experimental investigations have provided insights into the morphology of the vapor layer. As elucidated in Fig. 3(c), the curvature and height of the vapor layer and the non-axisymmetric interface fluctuations of water droplets were measured by fringe encoding via laser-light interference and high-speed imaging techniques (Burton et al., 2012), revealing film thickness within the range of 10-100 µm. Fringes are most discernible in regions proximate to the center of the vapor layer and the narrowest annulus neck. Real-time visualization of the interfacial profile of vapor films can be achieved through ultrafast X-ray imaging (Lee et al., 2018). Notably, on a smooth metallic surface, the vapor layer of a droplet at several millimeters corresponds to an average thickness of 10-20 µm, as elucidated by a high-speed electrical approach (Harvey et al., 2021), dynamic fluctuations in the central vapor layer and around the neck region are evident and pivotal for drop propulsion, oscillations, and star shapes observed on high-temperature substrates. Moreover, surface roughness tends to induce various instabilities in the vapor layer beneath the Leidenfrost droplet (Aursand et al., 2018; Chantelot and Lohse, 2021; Zhao and Patankar, 2020). To facilitate more rapid collapse of the vapor film, the critical thickness of the vapor film on a rough surface must not exceed the combined effect of surface roughness and the critical thickness observed on a smooth surface (Wakata et al., 2023).

The intricate nature of the vapor layer in the Leidenfrost effect, characterized by short temporal scales and multiple dimensions, can be effectively captured through multiphysics simulations, spanning computational fluid dynamics and molecular dynamics. The study of the underlying vapor film via the direct simulations using level set/arbitrary Lagrangian-Eulerian methods (Ge and Fan, 2005) and level set/ghost fluid methods (Villegas et al., 2017) is challenging, because of the multiscale characteristics of the Leidenfrost phenomenon. Addressing the full Navier-Stokes-Fourier equations throughout the entire computational domain, in conjunction with capturing the liquid-vapor interface, necessitates both high-density grids in the liquid and surrounding medium—particularly within the thin vapor layer and exceedingly small time steps to ensure stable and accurate solutions. Chakraborty et al. (2022) combined the lubrication approximation of vapor flow with the Navier-Stokes equations for inner flow in droplets and proposed a robust hybrid/multiscale computational model to capture the dynamics of impacting Leidenfrost droplets (Fig. 3(d)), such as the dynamic chimney instability. Notably, this model enables the prediction that small drops will transition to dimple-less droplets. The key advantage lies in its efficiency, as it solely requires meshing of the liquid domains while treating the vapor as a boundary condition for the droplet. Kinetic theory or molecular scale studies have found that the collapse of the vapor film may come from the balance failure between thermocapillary forces and vapor thrust stabilization (Aursand et al., 2018), the rapid growth of well-defined perturbations (such as gas inertia) within a few milliseconds (Harvey and Burton, 2023), or van der Waals interactions between the bulk liquid and the solid substrate across vapor layer (Zhao and Patankar, 2020). Nevertheless, the precise conditions for the collapse of vapor layers suspended on micro-nano pillars or porous materials remain poorly understood, highlighting a lack of experimental methodologies capable of swiftly disrupting vapor films and enhancing heat transfer efficiency.

2.3 Phase-change heat transfer theories

Efforts aimed at mitigating the interfacial Leidenfrost phenomenon and enhancing thermal management efficiency should adhere to the following principles. Firstly, strong wicking ability should be ensured to enlarge liquid-solid contact area and increase the uniformity of liquid distribution. Next, sustaining nucleation sites is crucial to facilitating adequate phase-change heat transfer. Lastly, to further increase liquid-solid contact, the presence of adequate channels or a high detachment frequency is vital to ensure prompt vapor bubble evacuation. Bubble nucleation is pivotal in boiling heat transfer processes, exerting a significant influence on heat transfer efficiency by affecting the nucleation efficiency, growth rates, and bubble detachment frequencies from a heated surface.

Typically, the nucleation of a vapor bubble (Fig. 4(a)) on a heated surface begins with the saturated liquid (Cho and Wang, 2019) and involves overcoming an energy barrier, which can be expressed by the classical nucleation theory

(Zhang et al., 2022), $R = \frac{2\gamma}{\Delta G \rho_v}$, here γ is the surface tension, ΔG is combined free energy, and ρ_v is the density of the

vapor. A bubble nucleated on a rough surface involves understanding the interaction between the liquid and the interfacial structure. On the one hand, the rough surfaces creating more micro-scale cavities or protrusions make bubble nucleation more readily. On the other hand, the rough surface geometry may alter the Gibbs free energy associated with bubble formation (Gallo et al., 2021), $\Delta G = 16\pi\gamma^3/(3\Delta p^2(1-\cos\theta))$, where θ is the contact angle. For example, on an amphiphilic surface, a bubble nucleates in hydrophobic regions, while its lateral expansion is inhibited by the hydrophilic regions. Similarly, on a bi-thermally conductive surface, the nucleation site density, energy barriers and bubble dynamics can be modulated by exploiting heterogeneity thermal region. The bubble once formed exerts an interfacial Laplace pressure on the surrounding liquid (Jones et al., 1999), $\Delta p = 2\gamma/R$. In addition, the bubble removal frequency can be expressed as $f = \frac{u}{2\pi R}$ (Malenkov, 1971).

In a three-phase interface system in Fig. 4(b), a bubble grows on the surface of interfacial material as a result of heat conduction and exhibits a pendant shape with a height l_b (Tamvada et al., 2023). Heat transfer occurs within a thermal boundary layer around the growing bubble, which can be described using Fourier's law (Baron Fourier, 2003),

 $q = -\lambda \frac{\partial T}{\partial x}$, where q is the heat flux, λ is the thermal conductivity of the material, $\partial T/\partial x$ is the temperature gradient.

The largest thickness of the micro-layer is δ_0 and the temperature profile within the thermal boundary layer is linear. According to Utaka et al.'s research (Utaka et al., 2013), the δ_0 is expressed as $\delta_0(r_L) = C_0 r_L$, where C_0 is a constant that can only be determined by measurement. The temperature of the upper boundary of the micro-layer is the same as that of the saturated vapor inside the bubble, which is expressed as T_b . The temperature of the micro-layer's bottom boundary is T_{sw} . If the temperature of the heated surface T_s is fixed, the heat through the bubble is equal to $\lambda_1 \frac{(T_{sw} - T_s)}{l_b}$,

and the heat through the micro-layer is equal to $\lambda_s \frac{(T_{sw}-T_b)}{\delta_o/2}$, here λ_s and λ_l are thermal conductivity for surface and liquid, respectively. Once bubbles coalesce and form a vapor film (Fig. 4(c)), the heat transfer through liquids will fail, greatly impairing the heat transfer efficiency.

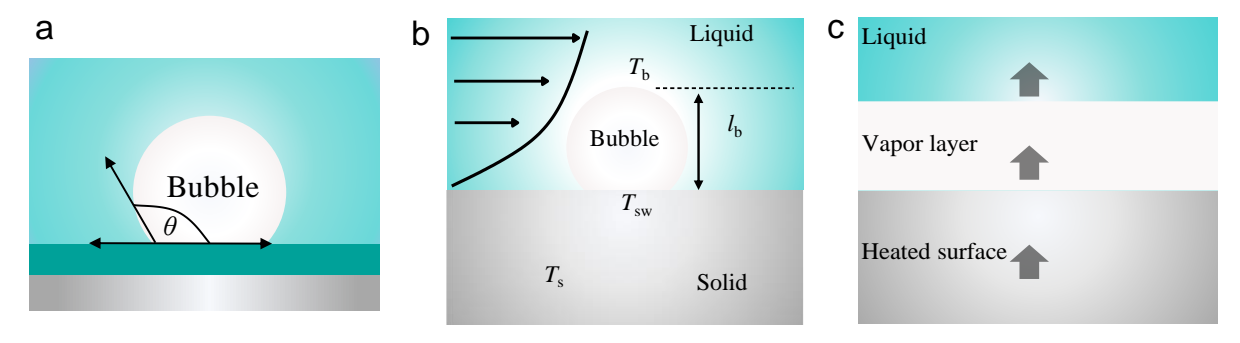


Fig. 4 Heat transfer model in different stages. a) Bubble nucleating on a smooth surface. b) Interfacial heat transfer of three-phase interfaces among the bubble, liquid and solid. c) Heat transfer through the vapor film.

3. Inhibition strategies of Leidenfrost effect

After hundreds of years of evolution, many strategies have been developed to suppress the Leidenfrost phenomenon. In this section, we will discuss how different approaches, including micro/nanostructures, fluid modifications, and external fields, inhibit the Leidenfrost effect as well as the associated underlying mechanisms.

3.1 Substrate structures and materials

Meticulously designed interface engineering is a promising avenue for mitigating the Leidenfrost phenomenon. In this section, we will examine the influence of micro/nanopillars, porous materials, and hierarchical heterogeneous structures on inhibiting the Leidenfrost effect, and particularly highlight their roles in modulating thermal dynamics, enhancing liquid retention, and enhancing vapor evacuation.

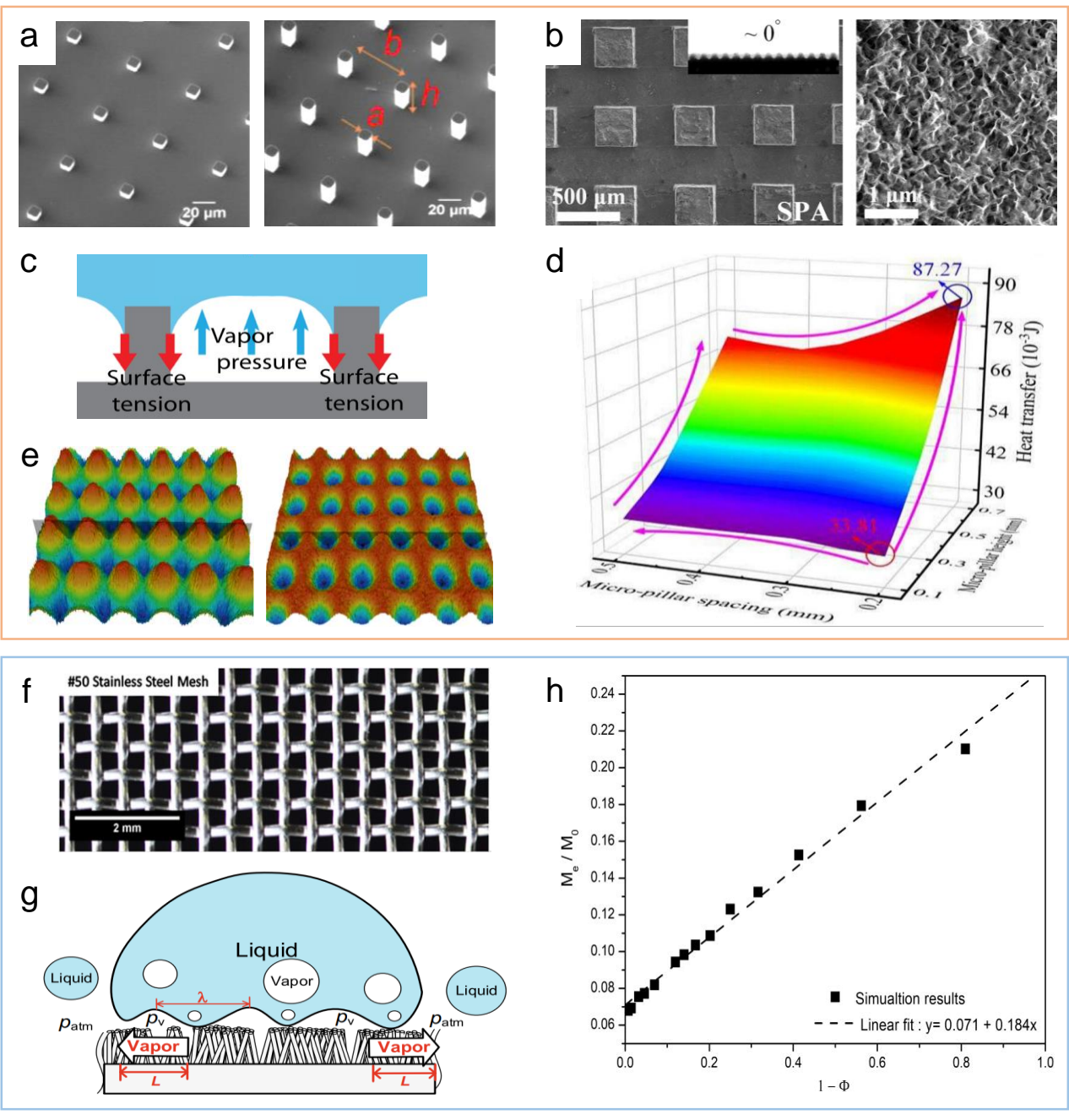


Fig. 5 Micro/nanopillars and porous materials for inhibiting the Leidenfrost effect. a) Micro/nano pillars with different spacing and heights (Prasad et al., 2021). b) Micro/nano hierarchical surface (Du et al., 2023b). c) Levitation mechanisms of droplets on micro/nanopillars (Kwon et al., 2013). d) Synergistic effects of the height and spacing of micro-pillars in heat transfer (Zhai et al., 2024). e) Pillar-like structure (Del Cerro et al., 2012). f) Stainless steel mesh (Geraldi et al., 2016). g) Levitation mechanisms of droplets on nanowires (Sahoo et al., 2020). h) Normalized droplet evaporated mass M_c/M₀ versus surface solid fraction 1-Φ, and the linear fitting function (dashed line) (Wang et al., 2022).

3.1.1 Micro/nanopillar structures

Micro/nanopillar structures have shown reliable performance in inhibiting the Leidenfrost effect and improving heat dissipation on high-heat-flux surfaces (Kim et al., 2011; Talari et al., 2018). Figure 5 delineates various micro/nanopillars alongside the mechanisms that impede the Leidenfrost effect. For example, the LFP increases from 270 °C on a smooth silicon substrate to 507 °C on a substrate with tall and sparse micropillars (Fig. 5(a)), due to the increased droplet-substrate contact areas, additional pinning effects, and combined boiling modes along the pillar height (Prasad et al., 2021). Leveraging the potent capillary effect for liquid wicking and the heightened permeability of micro/nanocavities for vapor flow (Du et al., 2023b), dynamic LFPs exceeding 500 °C were achieved on micropillar arrays (Fig. 5(b)). As

demonstrated by a parametric study (Kwon et al., 2013), counterintuitively, the sparser pillar substrate actually resulted in an increased LFP rather than the denser pillar structure. Both bubble nucleation sites and increasing vapor flow resistance increase with the increase of the spatial density of micro/nanopillars on the substrate. According to the quantified studies from Kim et al. (2019), on surfaces featuring low spatial density micropillars, the impact of nucleation-assisted agitation on droplet dynamics is minimal for simplicity. Conversely, on surfaces with high spatial density micropillars, elevated friction and vapor pressure lead to reduced LFPs. Notably, on surfaces with a medium spatial density of micropillars, the time duration before droplet rebound increases significantly, with nucleation activities at the liquid-solid interfaces affecting droplet stability, thereby maximizing the LFP. In a similar vein, Kim (2020) measured the LFP on circular micropillars with pitches ranging from 15 to 1000 µm and found the maximum LFP at a pitch of 120 μm. The increase in LFP facilitated by micro/nanopillars results from the interplay between capillary forces exerted by the pillars and the increased hydrodynamic resistance to vapor flows in the gaps between the pillars (Fig. 5(c)). Aiding the volume of fluid (VOF) model and an optimized evaporation model via the computational fluid dynamics (CFD) method, Zhai et al. (2024) ascertained that, regardless of whether the surface temperature was proximity to the LFP, heightened pillars significantly enhance heat transfer, indicating that the critical micropillar spacing for optimal heat transfer shifts to a smaller value from a larger one. Careful selection of micropillar parameters can significantly reduce the Leidenfrost effect, thereby elevating heat transfer efficiency (Fig. 5(d)). Notably, the heat transfer performance is improved by 44.89% at a surface temperature of 413.15 K and by 92.22% at 573.15 K.

From another perspective, micro/nanopillars may also confine LFPs by strengthening the flow resistance of escaping vapor. For instance, the LFP on the surfaces with dense topographies of micropillars and microholes (Fig. 5(e)) is reduced by approximately 105 °C and 85 °C. Because the dense microstructure provides more bubble nucleation sites and facilitates vapor formation, while simultaneously limiting the available space for gas evacuation (Bernardin and Mudawar, 2002). Likewise, analogous trends were identified on micropatterned surfaces (DdCerro et al., 2012; Tran et al., 2013).

3.1.2 Porous materials

[DOI: 10.1299/jtst.24-00360]

Several porous materials have displayed remarkable efficacy in mitigating the Leidenfrost effect, including porous ceramics (Avedisian and Koplik, 1987), carbon nanotubes (Kim et al., 2013), nanowire arrays (Sahoo et al., 2020), nanofibers (Nair et al., 2014), and graphene (Lim et al., 2022). On a mesh surface (Fig. 5(f)), the liquid only contacts mesh wires, whilst bridging wire gaps at the action of the surface tension of liquids, implying that the heat flux required to generate a supporting vapor layer in the Leidenfrost state must be transferred exclusively through the contact area between the liquid and solid wires. Consequently, generating a continuous vapor layer and maintaining the Leidenfrost state require elevated temperatures that increase with open areas (Geraldi et al., 2016). In general, the most notable advantages of porous materials in increasing LFP are promoting capillary wicking and pinning effects for liquid droplets, providing spacious escape paths for the vapor flow by porous structures, decreasing vapor pressure levitating droplets, and thus preventing the establishment of a stable vapor layer (Fig. 5(g)). A cost-effective and easily fabricated superhydrophilic nickel foam exhibits rapid droplet penetration within tens of milliseconds, elevating the dynamic Leidenfrost point beyond 500 °C (Du et al., 2023a). Compared to the nickel surface, the nickel foam nucleates at high superheat and induces a heat flux that is an order of magnitude higher. These remarkable features can be attributed to the superhydrophilic property promoting capillary wicking, the high porosity reducing effective thermal conductivity, and the large pore diameter enhancing permeability. Droplet penetration is governed by inertial and capillary forces at low and high superheat levels, respectively, with moderate pore diameters proving more conducive to facilitating droplet penetration. The pore diameter plays a negligible role at high surface temperatures due to the trade-off between effective thermal conductivity and specific surface area. Nanoporosity was found to exert a more pronounced impact on the Leidenfrost phenomenon than wettability (Kim et al., 2011). Compared to nonporous surfaces, bubbles nucleate more facilely on nanoporous surfaces and grow rapidly in the highly superheated liquid, thus enhancing the LFP. To identify the factors that significantly contribute to increasing the LFP of porous materials, Lee et al. (2019) detected various factors of sintered porous wick surfaces and found that the LFP and the heat transfer performance during film boiling were primarily dominated by surface thermal effusivity. With the help of multi-phase thermal lattice Boltzmann method, Wang et al. (2022) explored the effects of the Weber number and porous plate configurations (temperature, flat plate, porous plate, and varying pore intervals) on Leidenfrost droplet dynamics and heat transfer performance. Elevated temperature, larger Weber numbers, and reduced pore intervals can expedite droplet pancake bouncing due to the additional lift force

imparted by vapor pressure evaporation within pores. Furthermore, the evaporated droplet mass increases linearly with the impacting Weber numbers and the plate opening fractions (Fig. 5(h)).

3.1.3 Heterogeneous structures

Heterogeneous structures have been widely explored in the fields of thermal management (Chen et al., 2011; Cheng et al., 2021; Hou et al., 2015; Sun et al., 2022) due to the remarkable synergistic effects exhibited by zones with markedly distinct mechanical and physical properties. In recent years, there has been a gradual exploration of several multiscale heterogeneous structures for mitigating the Leidenfrost effect. These structures effectively combine the robust liquid-wicking capabilities of porous materials with the ample vapor escape paths offered by micro/nano-pillars.

The initial venture into homogeneous architectures involved the integration of two corrugated copper meshes and multiple layers of copper nanoparticles (Saj adi et al., 2017). This configuration successfully distinguishes the liquid infiltration induced by nanoparticles and the vapor flow pathways facilitated by copper meshes, effectively alleviating the Leidenfrost phenomenon at temperatures below 220 °C while maintaining high heat dissipation capacity. The second representative multiscale homogeneous structure (Farokhnia et al., 2017) allows the suppression of the Leidenfrost effect even at a substrate temperature of up to 570 °C by j ointing a superhydrophilic nanomembrane to the top of silicon micropillars with high thermal conductivity. The cooling droplet is stabilized against the hot solid owing to capillary forces created by the nanomembrane, while the resulting vapor is flowing radially outward, thus permitting the independent control of these two forces. Crucially, this decoupled hierarchical structure delivers exceptional heat dissipation capabilities at elevated surface temperatures. It is worth noting that the micropillar height should be at least 95 µm. As previously mentioned, if the surface feature is thinner than the vapor film, then the surface feature will merely increase the shear resistance of vapor flows, resulting in decreasing LFP (Kim et al., 2011).

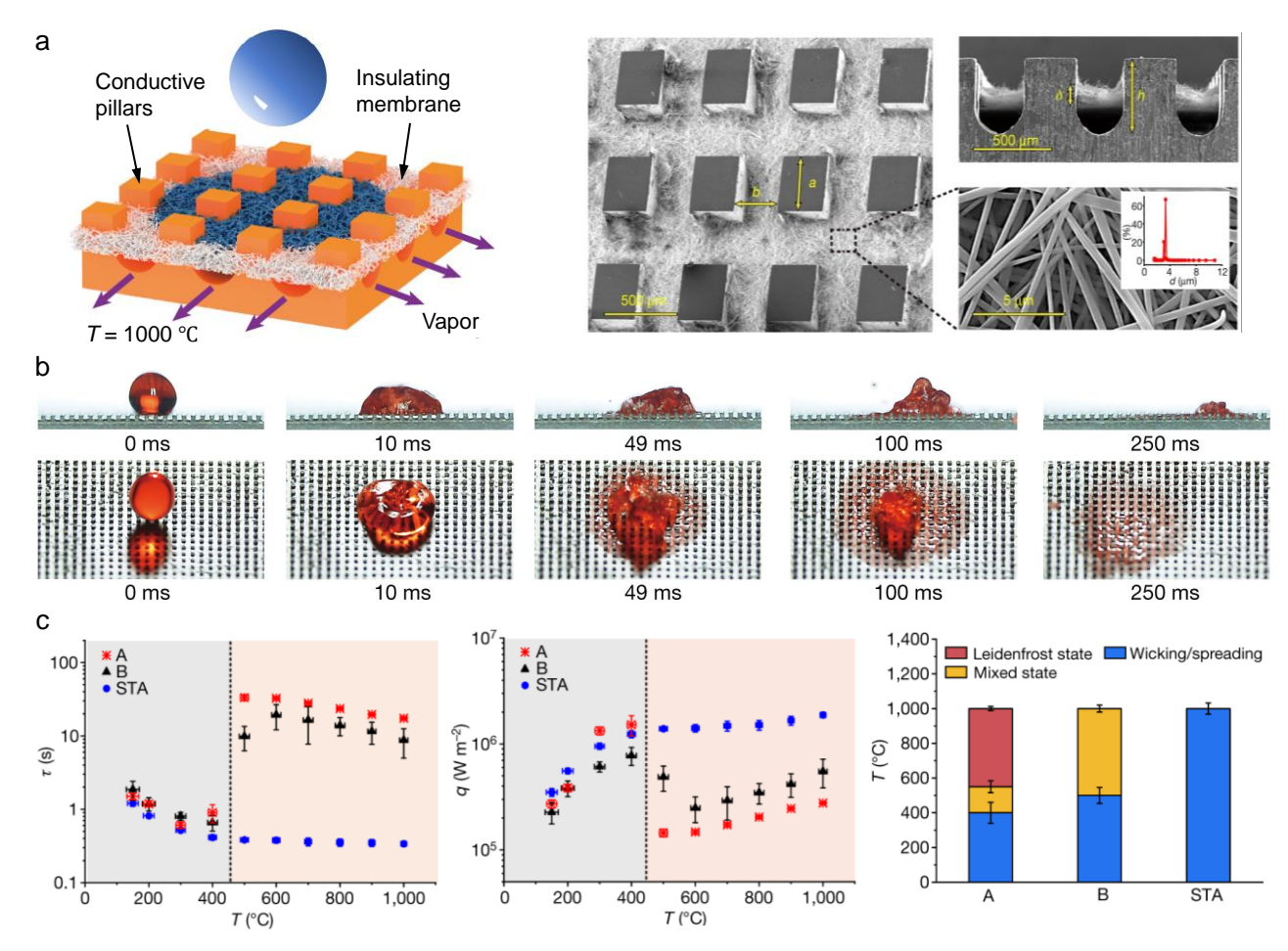


Fig. 6 Multiscale heterogeneous structure STA for suppressing the Leidenfrost effect (Jiang et al., 2022). a) Composition of structure thermal armor. b) High-speed camera images of a water droplet with a volume of 17 μl on STA at a temperature of 1000 °C. c) Lifetime τ, average heat flux, and phase diagram.

The third groundbreaking multiscale heterogeneous structure is the structural thermal armor (denoted as STA, see Fig. 6(a)) proposed by Jiang et al. (2022), which incorporates conductive steel pillars for bubble nucleation, embedded insulating porous membranes for rapid wicking and liquid spreading, and U-shaped channels for vapor evacuation. A standout feature of this STA lies in the use of heterogeneous materials with varying geometrical sizes, thermal conductivities, and wetting properties, culminating in a notable Leidenfrost point of 1150 °C, surpassing the previous benchmark by nearly 600 °C. This is the highest LFP recorded in current engineering fields, which may be further elevated by adopting materials with a higher melting point. Figure 6(b) presents the side and top views of water droplets with a volume of 17 µl contacting the sample STA at a temperature of 1000 °C, where neither a Leidenfrost state nor a mixed state is observed. At elevated temperatures, the lifetime of water droplets on the sample of STA is 50 times shorter than that on the sample of micropillar or the sample without vapor escape channels, while the heat flux is increased by approximately tenfold (Fig. 6(c)). This can be attributed to the larger nucleation areas provided by pillars, the enhanced liquid supply capacity from the insulated porous membrane to the conductive pillars, and the strong vapor evacuation ability of U-shaped channels beneath the insulating membrane. Furthermore, Jiang et al. (2022) undertook parameter optimization for the STA, scrutinizing factors such as the minimum height of vapor channels, droplet penetration depth, maximum membrane pore size, wicking duration, and cooling time of porous membranes. The researchers deduced that the optimal pillar density for STA to achieve the highest heat flux is 0.25. To date, there remains a notable research gap concerning the impact of heterogeneity in hierarchical heterostructures on the Leidenfrost effect.

3.2 Liquid modifications

Liquid modification refers to altering the properties of liquids, such as viscosity, surface tension, and latent heat of vaporization, to affect evaporation and heat transfer. We summarize the specific effects of various liquid modification approaches, including polymer additives, alcohol additives, surfactants, nanoparticles, and nanobubbles, thereby refining droplet interactions and thermal responses.

3.2.1 Liquid additives

Alcohol is the first notable category of liquid additives, primarily relying on varying concentrations to modulate the overall surface tension of droplets, which allows for control over the changes in Leidenfrost temperature. As illustrated in Fig. 7(a), the concentration of the alcohol additive itself has a minimal effect on the dynamic LFP (Cai et al., 2023b). However, the influence of the concentration of the alcohol additive on the dynamic LFP of alcohol-water mixture droplets is significantly greater than that of pure water or pure alcohol. This is because the addition of a small portion of alcohol additive droplets lowers surface tension, enhances liquid spreading, decreases bubble departure diameter, increases bubble departure frequency, and retards bubble coalescence. These factors collectively contribute to a substantial enhancement in droplet LFP, achieving the highest value at approximately 450 °C. This study highlights the significant potential at alcohol additives in enhancing droplet LFP.

Another kind of liquid additive is surfactant, which exhibits a substantially beneficial effect on elevating LFPs. For instance, high alcohol surfactants (HAS) of 1-octanol and 2-ethylhexanol can actually increase the dynamic LFPs up to 450 °C (Chen et al., 2018a). This phenomenon stems from the reduction in droplet surface tension, resulting in a larger diameter but thinner thickness after droplet spreading. Consequently, bubble coalescence becomes more challenging, thereby hindering the vapor layer formation and rendering the Leidenfrost state more unstable. A direct correlation between the surfactant concentration and LFP is delineated in Fig. 7(b), where LFP monotonically rises with the concentration of sodium dodecyl sulfate (SDS), up to 280 °C. This escalation is because the inclusion of the solute counterpart amplifies the thermal Marangoni instability, leading to a distinctively distorted droplet interface induced by thermal- and solute-capillary perturbations (Prasad et al., 2022). Conversely, ionic surfactants could significantly decrease LFP due to the ability of nonpolar chains of surfactant monomers to anchor bubbles on surfaces for in-situ growth and could facilitate adjacent bubble coalescence to form vapor layers (Zhang et al., 2020).

Different dynamic behaviors of polymer droplets may impose an influence on the LFP by altering contact time and thermal conduction. Firstly, polymer additives may increase the droplet viscosity and prevent fragmentation. For example, polyethylene oxide (Bertola, 2009) was found to reduce the maximum spreading diameter and enhance the rebound behaviors of droplets. Dhar et al. (2020) identified a much clearer relationship between polymer additives and LFP. Dissolved polyacrylamide droplets exhibit a delayed Leidenfrost effect (higher LFP) than pure water until reaching a

concentration of 1000 ppm. Conversely, mixture droplets at a concentration of 1500 ppm display a substantially lower LFP than pure water. This could be summarized as high concentrations of polymer additives may over-increase the droplet viscosity, preventing droplets from adequate spreading and limiting contact areas required for effective heat transfer.

Industrial applications often require using multiple liquid additives to achieve optimal performance, which necessitates discussing more intricate scenarios involving multiple components and interactions (Sen et al., 2017; Sen et al., 2020). The first situation to be introduced is the spontaneous explosion of mixed droplets with a multitude of smaller secondary droplets. For instance, this behavior was observed in a mixture droplet of water, ethanol, and oil (Lyu et al., 2021) due to the preferential gasification of ethanol promoting oil microdroplet nucleation, leading to oil microdroplets enveloping water, thereby reducing vapor layer thickness (Fig. 7(c)). Another example concerns different droplets with different components and different boiling points. If two droplets with different boiling points are placed simultaneously on a hot surface, the droplet with a higher boiling point could work as a new heat source for the one with a lower boiling point, which may form a vapor layer between the two adjacent droplets, preventing their coalescence. This more complex phenomenon is called the triple Leidenfrost effect (Pacheco-Vazquez et al., 2021). However, the interactions and the uneven temperature distributions within droplets of differing compositions render the investigation more challenging, necessitating further exploration and elucidation.

3.2.2 Dissolved gas additives

When considering the effect of dissolved gases on the LFP of droplets, conflicting viewpoints emerge. One school of thought posits that augmenting nanobubble concentrations can boost LFPs. An illustrative example of delaying the Leidenfrost effect involves the dispersion of significant oxygen nanobubbles (ranging from 100-200 nm) within fluid droplets, resulting in an increase in LFPs to 320 °C (Vara Prasad et al., 2022). The crucial mechanisms behind this effect can be traced to the rewetting properties due to the presence of dispersed nanobubbles and possible microscale gas layer formed between solid-liquid interfaces. Additionally, in the nucleate boiling regime, carbon dioxide (CO₂) which is highly soluble in water could help to increase the heat transfer of droplets due to the prevention of the coalescence of vapor bubbles (Cui et al., 2001). However, as the surface temperature approaches the LFP, the dissolved CO₂ escapes from underneath droplets, preventing droplets from contacting the substrate and suppressing heterogeneous nucleation, thereby reducing the heat transfer between droplets and hot surfaces.

Quite different from the previous perspective, the significant complete degassing was revealed to be necessary for highly effective boiling heat transfer by molecular dynamics simulations (Situ et al., 2024). As the temperature rises, the dissolved air is released from the water and is adsorbed on solid surfaces, forming an interfacial air layer. Hence, instead of bubble departure, the Leidenfrost phenomenon manifests, further resulting in heat transfer deterioration. This negative effect of the interfacial gas layers can be reduced by high pressure.

3.2.3 Nanoparticle additives

Dispersed nanoparticle additives affect the Leidenfrost effect via a different mechanism, promoting intermittent solid-liquid contact and impeding the formation of the vapor layer. For instance, the optimal loading of TiO₂ nanoparticles has elevated the LFP to 300 °C while drastically reducing droplet lifetime by an order of magnitude (Paul et al., 2020). This can be explained by the deposition of nanoparticles by creating uniquely random porous structures on thermal substrates, which disrupts the Leidenfrost state and generates additional capillary wicking (Fig. 7(e)). Such an increase in LFPs of nanofluid droplets is also restricted by the concentration, materials, and shapes of dispersed nanoparticles, which increases the operational difficulty. Ulahannan et al. (2021) anticipated the impact of both spherical and cylindrical Al₂O₃ nanoparticles, revealing that the LFP of nanosphere-water and nanorod-water mixtures is lower than those of deionized water. The disparity in LFP was attributed to the heightened heat flux and the vapor formation induced by high-conductivity metal nanoparticles. In conclusion, an appropriate amount of well-shaped nanoparticles may effectively augment the LFP of mixed droplets.

In sharp contrast, one possible complex scenario is that a frozen disk placed on a sufficiently hot surface directly transitions from the solid to the gaseous state, resulting in an increment of LFP of approximately 400 °C over liquid water droplets (Edalatpour et al., 2022). This three-phase Leidenfrost state is also possible for other substances besides water, as long as the pressure exceeds their triple point, which is encouraged as an avenue of future research.

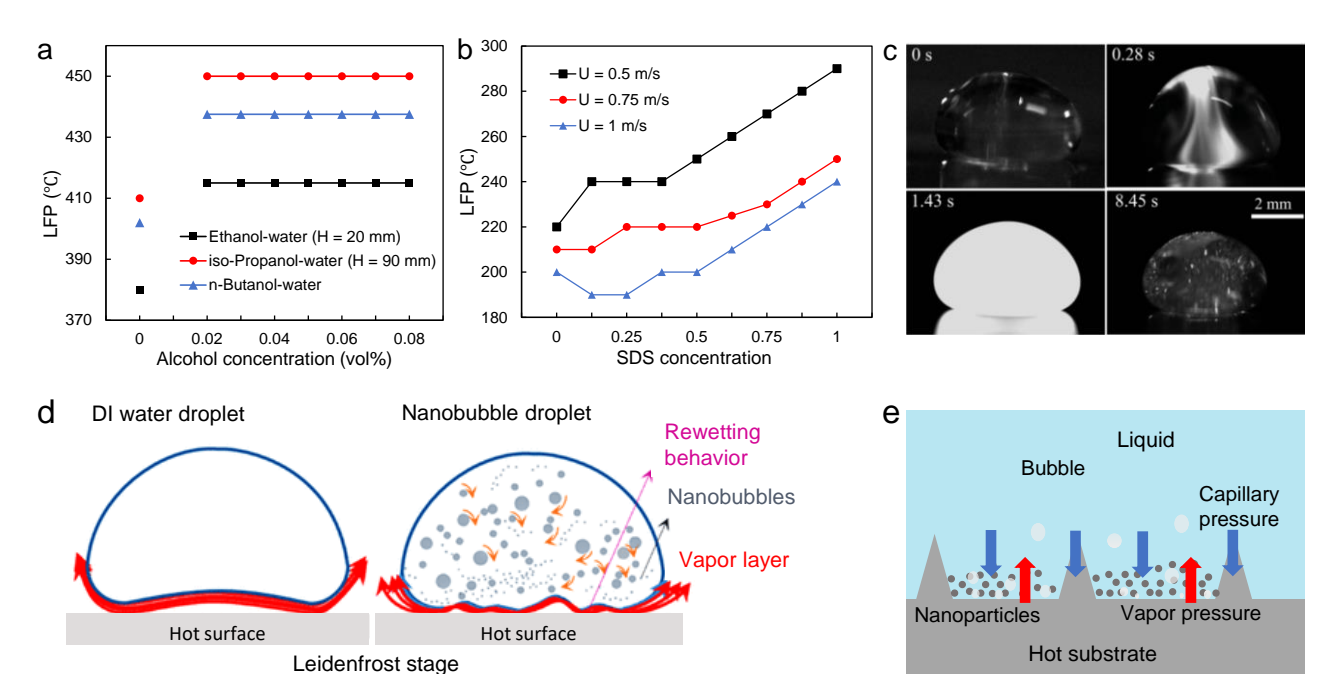


Fig. 7 Effects of fluid modifications on inhibiting the Leidenfrost effect. a) LFP at different alcohol concentrations (Dhar et al., 2020). b) LFP at different SDS concentrations (Prasad et al., 2022). c) Multicomponent additives (Lyu et al., 2021).
d) Enhancement mechanism of nanobubble additives (Vara Prasad et al., 2022). e) Enhancement mechanism of nanoparticle additives (Paul et al., 2020).

3.3 Active technologies

Applying external fields presents a viable solution to effectively mitigate the Leidenfrost effect (Fig. 8). In certain industrial applications, such as the combustion chambers of turbomachinery, it is often challenging and impractical to treat heat transfer surfaces through structural modifications or chemical treatments. External fields—including electric, pressure, gravitational, magnetic, and acoustic fields—can exert a strong inhibitory effect by driving the liquid back to a nucleate boiling state or modifying the shape of vapor layer, thereby ensuring continuous and efficient heat transfer.

3.3.1 Electric field

The most frequent method of suppressing the Leidenfrost effect using an external field is to apply an appropriate electrostatic field. The principle behind the electric field in suppressing the Leidenfrost effect lies in the interaction between electrostatic forces and capillary forces (Celestini and Kirstetter, 2012). As shown in Fig. 8(a), by increasing the voltage between the droplet and the substrate, the liquid is further attracted to the surface, reducing the thickness of the vapor layer and thereby enhancing the LFP (Ozkan et al., 2017). This technology is still partially effective even at an ultra-high temperature beyond 500 °C at a voltage of 90 V (Shahriari et al., 2014). However, achieving such high voltages is challenging in industrial settings. An alternative method is to increase the Weber number and thus adjust the ratio of impact velocity to electric field strength (Nazari and Pournaderi, 2019). The material properties of the heat transfer surface also influence the ability of electric fields to suppress the Leidenfrost effect. An electric field performed a better suppression effect on silicone oil surfaces and liquid metal surfaces than on ordinary solid surfaces (Shahriari et al., 2017), since the Leidenfrost droplets on a silicone oil surface can fully penetrate into the substrate and transform into a thin liquid film. A more precise method targeting the three-phase contact line could also achieve a similar inhibitory effect. Wang and his team (2024) significantly shortened droplet lifespan at least ten times on superhydrophilicity high-temperature surfaces by generating air discharge to increase the free energy near the three-phase contact line and combining electromechanical force to reduce contact angle. Different from the direct-current fields adopted in previous studies, high-frequency alternating electric fields would be completely negated, making it impossible to suppress the Leidenfrost effect (Lu et al., 2021).

3.3.2 Magnetic field

Under different magnetic field conditions, the Leidenfrost effect can manifest in two forms—suppression or induction. For example, to suppress the Leidenfrost effect, suspended magnetic ferrofluid droplets can be forcefully pressed onto an overheated surface using a non-uniform magnetic field. This method can reduce evaporation time to about one-third compared to droplets without a magnetic field (Kichatov et al., 2023). In contrast, applying a magnetic field in a different manner, specifically above the heat exchange surface, can enhance the Leidenfrost effect of ferrofluid (D'Angelo et al., 2019). The biggest advantage of using magnetic fields to suppress the Leidenfrost effect, compared to other methods, lies in their ability of operating in ultra-low-temperature industrial environments. As illustrated in Fig. 8(b), a magnetic field could be used to manipulate oxygen droplets placed on a heated surface, displaying a deformation characterized by capillary length (Piroird et al., 2013), which has profound significance for aerospace engineering, particularly for the antennas of deep space communication satellites that often operate in ultra-low temperature and zero-gravity environments.

Additionally, high-frequency sound waves offer an alternative technique to suppress the Leidenfrost effect without altering liquid properties and heat transfer surfaces. As illustrated in Fig. 8(c), as the excitation frequency increases, strong capillary waves are induced in the vicinity of liquid-gas interfaces and cause the droplet to contact with heated substrates, ultimately terminating the Leidenfrost effect (Ng et al., 2016).

3.3.3 Ambient pressure

Suppressing the Leidenfrost effect using electric or magnetic fields has a common and evident drawback: They do not interact effectively with uncharged or non-magnetic droplets. As such, changing the ambient pressure has been a reliable alternative. Experimental data indicated that the LFP increases with increasing pressure at both sub-atmospheric and above-atmospheric pressures (Orejon et al., 2014). The increase in ambient pressure results in thinner vapor layers and more liquid-solid contacts, elevating the Leidenfrost point to 440 °C (Van Limbeek et al., 2021) and intensifying the heat transfer rate in the film boiling regime (Kita et al., 2022). The improvement in the LFP may be associated with an elevated phase-transition temperature and a higher temperature limiting to sustain nucleate boiling in a high-pressure environment (Van Limbeek et al., 2021). This conclusion can be confirmed through experiments with various organic liquids, such as ethanol, FC-72, acetone, organic coolants, and liquid fuels. For instance, increasing the pressure from 1 to 20 bar can significantly increase the LFP of n-decane as much as 250 °C (Chausalkar et al., 2020), as shown in Fig. 8(d). A high-pressure environment can reduce the production of volatile components in fuels, making the formation of a vapor layer more difficult (Chausalkar et al., 2021).

3.3.4 Ambient gravity

Studying the variations of the Leidenfrost effect in different gravitational environments is of significance for the aerospace industry because heat exchange on space stations must bee carried out in microgravity or even zero-gravity conditions. Notably, the nucleate boiling of water and n-heptane droplets on a heated stainless-steel surface was unaffected by the reduction of gravity, but stable film boiling could not be maintained since droplets were pushed away from the surface by the vapor pressure beneath droplets (Qiao and Chandra, 1996). In such a situation, this characteristic can enhance water collection in the low-gravity environment of space stations (Rasheed et al., 2020), a 98% water recovery (Fig. 8(e)) was achieved by combining liquid-gas separation, nanoscale optical sterilization, and Leidenfrost distillation, increasing purified water by 18% over previous experiments. Additionally, understanding the Leidenfrost phenomenon under super-gravity conditions—such as the significant overloads experienced by propellers and fuel during rocket launches—is critical for understanding heat transfer behavior. However, as shown in prior experiments and analyses (Maquet et al., 2015), the LFP at 25-fold gravity is only about 15 °C higher than that at 1 gravity, indicating a minimal impact of high gravity on the LFP.

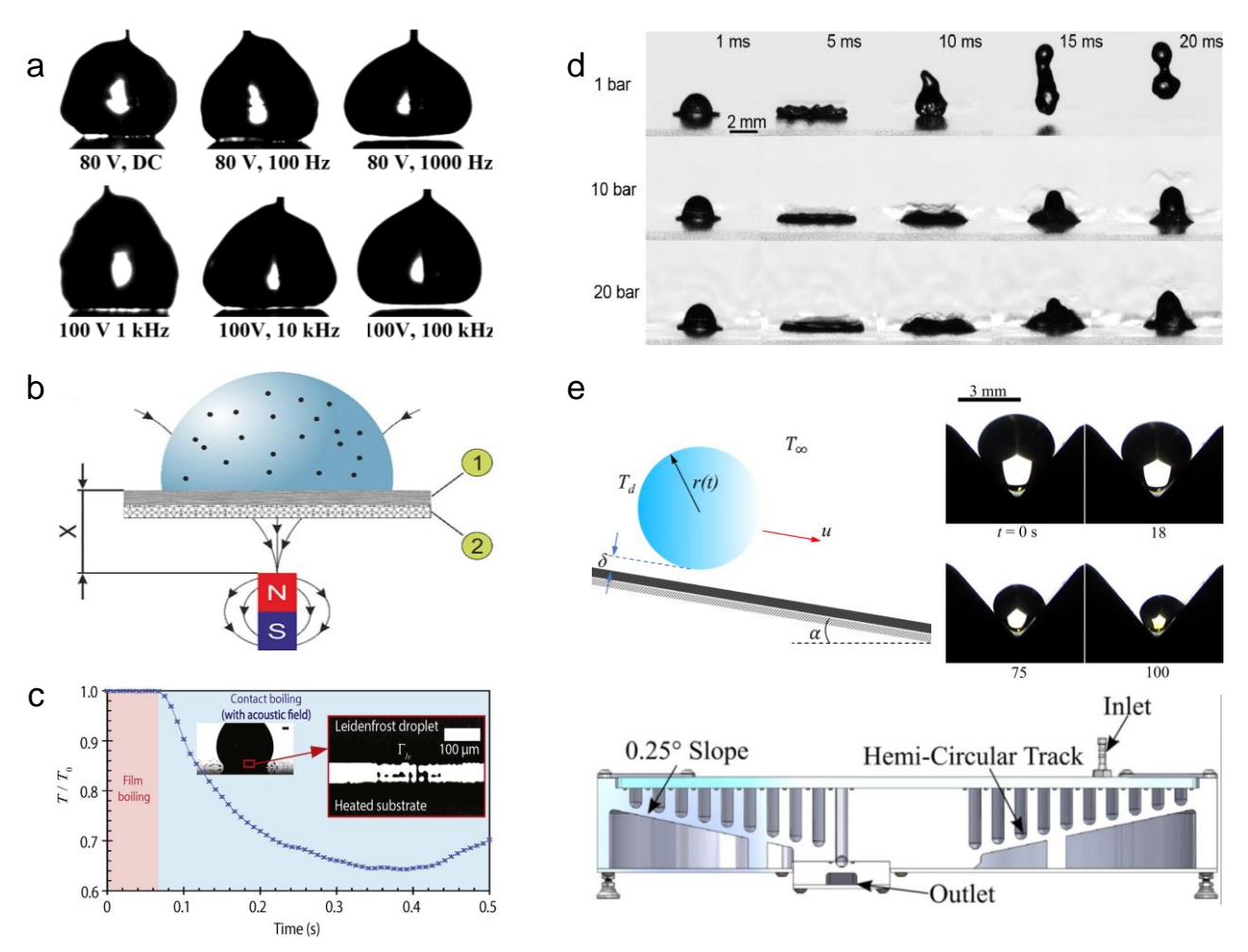


Fig. 8 Effects of external conditions on inhibiting the Leidenfrost effect. a) Electric fields (Ozkan et al., 2017). b) Magnetic field (Kichatov et al., 2023). c) Acoustic field (Ng et al., 2016). d) High-pressure environment (Chausalkar et al., 2020). e) Different gravity condition (Rasheed et al., 2020).

3.4 Comparison and discussion

Figure 9(a) summarizes the recent developments of the LFP, ranging from 200 °C to 1150 °C, in relation to substrate materials and configurations, liquid modifications, and external factors. The structural thermal armor developed by Jiang et al. (2022) exhibits the highest LFP of 1150 °C recorded to date. In contrast, both liquid modification, for instance, attains a peak LFP of approximately 450 °C (Cai et al., 2023a; Chen et al., 2018a), and an electric field can elevate the LFP to around 500 °C through an increase in voltage (Ozkan and Bahadur, 2020).

Figure 9(b) illustrates the heat flux of various ultra-high-temperature surfaces before the onset of the Leidenfrost effect in relation to LFP. Jiang et al. (2022) demonstrated that the phase-change liquid cooling of the structural thermal armors was still effective at 1150 °C, with a heat flux roughly ten times that of ordinary micropillar substrates. The interfacial electric fields can attract liquid toward the surface and prevent drying out, enabling a heat dissipation capability surpassing 500 W/cm² at temperatures above 500 °C (Shahriari et al., 2014). The decoupled hierarchical structure (Farokhnia et al., 2017) delivered a notably high heat dissipation capacity by independently adjusting capillary pressure and dewetting vapor pressure, albeit there is ambiguity regarding the heat flux calculation methodology in this study. While the cost-effective and readily manufacturable superhydrophilic nickel foams trigger a tenfold increase in heat flux compared to conventional solid nickel surfaces (Du et al., 2023a), while this study focused on impinging Leidenfrost droplets. Evidently, within the realm of interfacial engineering studies on the Leidenfrost phenomenon, statistical data on the conventional heat flux metric are lacking, emphasizing the heightened desirability of high heat flux at elevated temperatures.

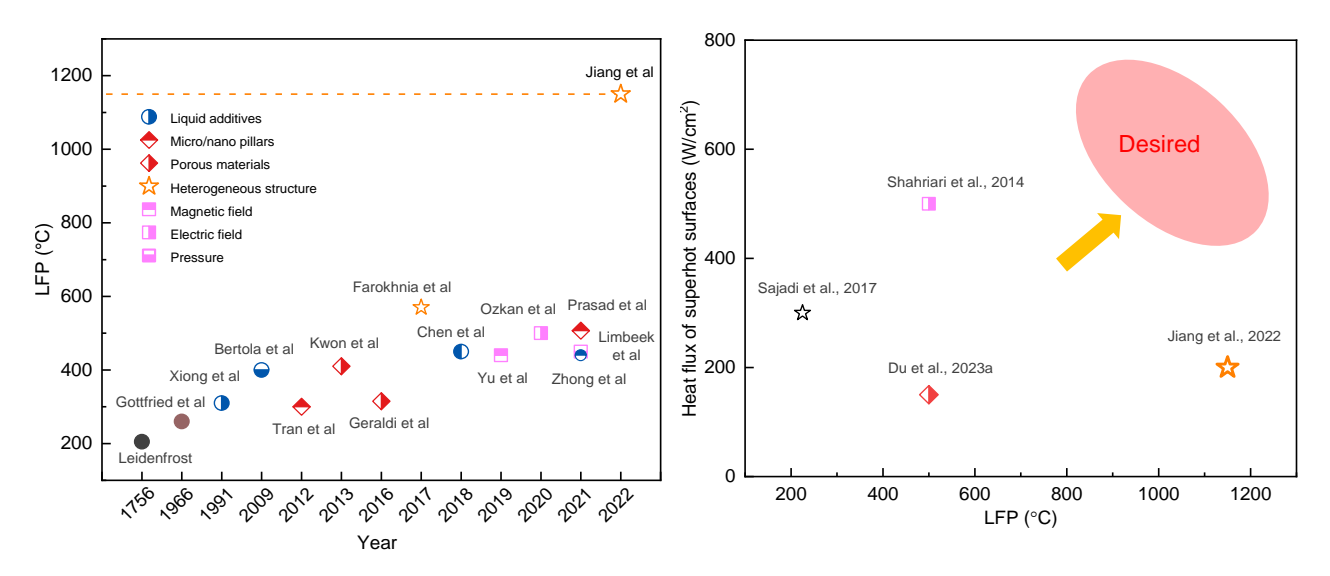


Fig. 9 Comparison of LFP and heat flux. a) Development history of LFP. b) Heat flux on high-temperature surfaces before the Leidenfrost effect, versus LFP.

4. Conclusion and perspective

In this review, we not only endeavor to explore classical theories and a holistic understanding of the Leidenfrost phenomenon, but also to examine cutting-edge strategies related to surface materials and structures, droplet modification, and external fields to improve the Leidenfrost point and heat transfer efficiency of high-temperature surfaces. Key conclusions and future prospects can be summarized as follows.

From a fundamental standpoint, mitigating the Leidenfrost effect necessitates a delicate trade-off between the liquid-wettability and the vapor outgassing rate. Specifically, effective strategies for inhibiting the Leidenfrost effect should focus on facilitating the thinning or collapse of vapor films, thereby increasing solid-liquid contact and ultimately maximizing heat transfer performance. Structural enhancements emerge as a paramount and straightforward method to boost the LFP. Micro/nano-pillars and porous configurations play critical roles in elevating the Leidenfrost point by enhancing vapor dissipation and reinforcing liquid While multi-scale heterogeneous hierarchical structures bolster LFP by both elevating exhaust rates and enhancing wettability, they have achieved an impressive LFP of 1150 °C to date. Moreover, diverse liquid modification techniques, including polymer additives, alcohol additives, surfactants, nanoparticles, and dissolved gases, can imbue droplets with various properties. Notably, alcohol additives and surfactants stand out for their ability to enhance Leidenfrost points by elevating bubble detachment frequency and delaying vapor layer formation, exhibiting reliable and broad effectiveness across concentrations. Finally, external fields can directly exert powerful suppressive effects on the Leidenfrost phenomenon, forcing liquid back to nucleate boiling or adjusting the vapor layer morphology, which makes it particularly valuable in engineering applications where direct modifications or chemical treatments for substrates are not feasible.

Despite notable progress in recent decades, several fundamental challenges persist. Precise observation of the vapor film on microstructures necessitates advanced experimental techniques, while the complex gas-solid-liquid interactions at multiple scales pose a daunting challenge for developing reliable numerical simulation methods for the Leidenfrost phenomenon. Additionally, the quest for more resilient materials capable of withstanding extreme temperatures to effectively mitigate the Leidenfrost effect remains ongoing. Notably, ultra-high-temperature ceramics exhibit exceptional superhydrophilicity and superior thermal conductivity (Lin et al., 2023; Wyatt et al., 2023). Inhibiting the Leidenfrost effect in confined environments like integrated circuits and nuclear reactors is still a formidable challenge. Ultimately, the strategies for mitigating the Leidenfrost effect hold significant promise cross an inclusive spectrum of applications, spanning from low-temperature bioengineering (Li et al., 2018) to hydrogen production (Angulo et al., 2020).

Acknowledgements and conflicts of interest

We acknowledge financial support from the National Natural Science Foundation of China (Nos. T2293694, 52333015, 11215523), National Key Research and Development Program of China (No. 2023YFE0209900), Research Grants Council of Hong Kong (Nos. 15237824, SRFS2223-1S01, 11215523, N_PolyU5172/24), the Innovation and Technology Commission of Hong Kong (No. MHP/025/23), Meituan Foundation through the Green Tech Award, and Research, Academic and Industry Sectors One-plus Scheme (No. RAI/23/1/094A). All authors declare no competing financial or personal interests. Huaduo Gu and Mingyu Li contribute equally to this work.

References

- Agapov, R.L., Boreyko, J.B., Briggs, D.P., Srijanto, B.R., Retterer, S.T., Collier, C.P. and Lavrik, N.V., Asymmetric wettability of nanostructures directs Leidenfrost droplets, ACS Nano, Vol.8, No.1 (2014), pp.860-867.
- Angulo, A., van der Linde, P., Gardeniers, H., Modestino, M. and Fernández Rivas, D., Influence of bubbles on the energy conversion efficiency of electrochemical reactors, Joule, Vol.4, No.3 (2020), pp.555-579.
- Aursand, E., Davis, S.H. and Ytrehus, T., Thermocapillary instability as a mechanism for film boiling collapse, Journal of Fluid Mechanics, Vol.852, (2018), pp.283-312.
- Avedisian, C. and Koplik, J., Leidenfrost boiling of methanol droplets on hot porous/ceramic surfaces, International Journal of Heat and Mass Transfer, Vol.30, No.2 (1987), pp.379-393.
- Baron Fourier, J.B.J., The analytical theory of heat (2003), Courier Corporation.
- Berenson, P., Experiments on pool-boiling heat transfer, International Journal of Heat and Mass Transfer, Vol.5, No.10 (1962), pp.985-999.
- Bernardin, J.D. and Mudawar, I., A cavity activation and bubble growth model of the Leidenfrost point, Journal of Heat and Mass Transfer, Vol.124, No.5 (2002), pp.864-874.
- Bertola, V., An experimental study of bouncing Leidenfrost drops: Comparison between Newtonian and viscoelastic liquids, International Journal of Heat and Mass Transfer, Vol.52, No.7-8 (2009), pp.1786-1793.
- Biance, A.L., Clanet, C. and Quéré, D., Leidenfrost drops, Physics of Fluids, Vol.15, No.6 (2003), pp.1632-1637.
- Bouillant, A., Mouterde, T., Bourrianne, P., Lagarde, A., Clanet, C. and Quéré, D., Leidenfrost wheels, Nature Physics, Vol.14, No.12 (2018), pp.1188-1192.
- Bourrianne, P., Lv, C. and Quéré, D., The cold Leidenfrost regime, Science Advances, Vol.5, No.6 (2019), DOI:10.1126/sciadv.aaw0304.
- Burton, J., Sharpe, A., Van Der Veen, R., Franco, A. and Nagel, S., Geometry of the vapor layer under a Leidenfrost drop, Physical Review Letters, Vol.109, No.7 (2012), DOI:10.1103/PhysRevLett.109.074301.
- Cai, C., Chen, H., Liu, H. and Si, C., Effect of iso-propanol additive on the impact dynamics of a Leidenfrost water droplet, Applied Thermal Engineering, Vol.234, (2023a), DOI:10.1016/j.applthermaleng.2023.121326.
- Cai, C., Liu, H., Chen, H. and Si, C., Alcohol-induced elevation in the dynamic Leidenfrost point temperature for water droplet impact, International Journal of Heat and Mass Transfer, Vol.215, (2023b), DOI:10.1016/j.ijheatmasstransfer.2023.124483.
- Celestini, F. and Kirstetter, G., Effect of an electric field on a Leidenfrost droplet, Soft Matter, Vol.8, No.22 (2012), pp.5992-5995.
- Chakraborty, I., Chubynsky, M.V. and Sprittles, J.E., Computational modelling of Leidenfrost drops, Journal of Fluid Mechanics, Vol.936, (2022), DOI:10.1017/jfm.2022.66.
- Chantelot, P. and Lohse, D., Leidenfrost effect as a directed percolation phase transition, Physical Review Letters, Vol.127, No.12 (2021), DOI:10.1103/PhysRevLett.127.124502.
- Chausalkar, A., Kweon, C.B.M., Kong, S.C. and Michael, J.B., Leidenfrost behavior in drop-wall impacts at combustor-relevant ambient pressures, International Journal of Heat and Mass Transfer, Vol.153, (2020), DOI:10.1016/j.ijheatmasstransfer.2020.119571.
- Chausalkar, A., Kweon, C.B.M. and Michael, J.B., Multi-component fuel drop-wall interactions at high ambient pressures, Fuel, Vol.283, (2021), DOI:10.1016/j.fuel.2020.119071.
- Chen, H., Cheng, W.L., Peng, Y.H. and Jiang, L.J., Dynamic Leidenfrost temperature increase of impacting droplets containing high-alcohol surfactant, International Journal of Heat and Mass Transfer, Vol.118, (2018a), pp.1160-1168.
- Chen, M.Y., Jia, Z.H., Zhang, T. and Fei, Y.Y., Self-propulsion of Leidenfrost droplets on micropillared hot surfaces with

- gradient wettability, Applied Surface Science, Vol.433, (2018b), pp.336-340.
- Chen, X., Wu, J., Ma, R., Hua, M., Koratkar, N., Yao, S. and Wang, Z., Nanograssed micropyramidal architectures for continuous dropwise condensation, Advanced Functional Materials, Vol.21, No.24 (2011), pp.4617-4623.
- Cheng, Y., Wang, M., Sun, J., Liu, M., Du, B., Liu, Y., Jin, Y., Wen, R., Lan, Z., Zhou, X., Ma, X. and Wang, Z., Rapid and persistent suction condensation on hydrophilic surfaces for high-efficiency water collection, Nano Letters, Vol.21, No.17 (2021), pp.7411-7418.
- Cho, H.J. and Wang, E.N., Bubble nucleation, growth, and departure: A new, dynamic understanding, International Journal of Heat and Mass Transfer, Vol.145, (2019), DOI:10.1016/j.ijheatmasstransfer.2019.118803.
- Cui, Q., Chandra, S. and McCahan, S., The effect of dissolving gases or solids in water droplets boiling on a hot surface, Journal of Heat and Mass Transfer, Vol.123, No.4 (2001), pp.719-728.
- D'Angelo, C., Raufaste, C., Kuzhir, P. and Celestini, F., Ferrofluid Leidenfrost droplets, Soft Matter, Vol.15, No.29 (2019), pp.5945-5950.
- Del Cerro, D.A., Marin, A.G., Romer, G.R., Pathiraj, B., Lohse, D. and Huis In 't Veld, A.J., Leidenfrost point reduction on micropatterned metallic surfaces, Langmuir, Vol.28, No.42 (2012), pp.15106-15110.
- Dhar, P., Mishra, S.R., Gairola, A. and Samanta, D., Delayed Leidenfrost phenomenon during impact of elastic fluid droplets, Proceedings of the Royal Society A, Vol.476, No.2243 (2020), DOI:10.1098/rspa.2020.0556.
- Du, J., Li, Y., Wang, X. and Min, Q., Inhibiting the Leidenfrost effect by superhydrophilic nickel foams with ultrafast droplet permeation, ACS Applied Materials & Interfaces, Vol.15, No.34 (2023a), pp.41121-41129.
- Du, J., Li, Y., Wang, X., Wu, X. and Min, Q., Dynamics and heat transfer of water droplets impacting on heated surfaces: The role of surface structures in Leidenfrost point, International Journal of Heat and Mass Transfer, Vol.212, (2023b), DOI:10.1016/j.ijheatmasstransfer.2023.124241.
- Dupeux, G., Baier, T., Bacot, V., Hardt, S., Clanet, C. and Quéré, D., Self-propelling uneven Leidenfrost solids, Physics of Fluids, Vol.25, No.5 (2013), DOI:10.1063/1.4807007.
- Ebrahimi, K., Jones, G.F. and Fleischer, A.S., A review of data center cooling technology, operating conditions and the corresponding low-grade waste heat recovery opportunities, Renewable and Sustainable Energy Reviews, Vol.31, (2014), pp.622-638.
- Edalatpour, M., Cusumano, D.T., Nath, S. and Boreyko, J.B., Three-phase Leidenfrost effect, Physical Review Fluids, Vol.7, No.1 (2022), DOI:10.1103/PhysRevFluids.7.014004.
- Farokhnia, N., Sajadi, S.M., Irajizad, P. and Ghasemi, H., Decoupled hierarchical structures for suppression of Leidenfrost phenomenon, Langmuir, Vol.33, No.10 (2017), pp.2541-2550.
- Gallo, M., Magaletti, F. and Casciola, C.M., Heterogeneous bubble nucleation dynamics, Journal of Fluid Mechanics, Vol.906, (2021), DOI:10.1017/jfm.2020.761.
- Ge, Y. and Fan, L. S., Three-dimensional simulation of impingement of a liquid droplet on a flat surface in the Leidenfrost regime, Physics of Fluids, Vol.17, No.2 (2005), DOI:10.1063/1.1844791.
- Geraldi, N.R., McHale, G., Xu, B.B., Wells, G.G., Dodd, L.E., Wood, D. and Newton, M.I., Leidenfrost transition temperature for stainless steel meshes, Materials Letters, Vol.176, (2016), pp.205-208.
- Graeber, G., Regulagadda, K., Hodel, P., Kuttel, C., Landolf, D., Schutzius, T.M. and Poulikakos, D., Leidenfrost droplet trampolining, Nature Communications, Vol.12, No.1 (2021), DOI:10.1038/s41467-021-21981-z.
- Gu, H., Liang, D., Duan, P., Zhou, D. and Li, W., Aerothermal characteristics of thin double-wall effusion cooling systems with novel slot holes and cellular architectures for gas turbines, Aerospace Science and Technology, Vol.140, (2023), DOI:10.1016/j.ast.2023.108441.
- Harvey, D. and Burton, J.C., Hydrodynamic collapse of the Leidenfrost vapor layer, Physical Review Fluids, Vol.8, No.9 (2023), DOI:10.1103/PhysRevFluids.8.094003.
- Harvey, D., Harper, J.M. and Burton, J.C., Minimum Leidenfrost temperature on smooth surfaces, Physical Review Letters, Vol.127, No.10 (2021), DOI:10.1103/PhysRevLett.127.104501.
- Hou, Y., Yu, M., Chen, X., Wang, Z. and Yao, S., Recurrent filmwise and dropwise condensation on a beetle mimetic surface, ACS Nano, Vol.9, No.1 (2015), pp.71-81.
- Jiang, M., Wang, Y., Liu, F., Du, H., Li, Y., Zhang, H., To, S., Wang, S., Pan, C., Yu, J., Quere, D. and Wang, Z., Inhibiting the Leidenfrost effect above 1,000 °C for sustained thermal cooling, Nature, Vol.601, No.7894 (2022), pp.568-572.
- Jollans, T. and Orrit, M., Explosive, oscillatory, and Leidenfrost boiling at the nanoscale, Physical Review E, Vol.99, No.6 (2019), DOI:10.1103/PhysRevE.99.063110.

- Jones, S., Evans, G. and Galvin, K., Bubble nucleation from gas cavities—a review, Advances in Colloid and Interface Science, Vol.80, No.1 (1999), pp.27-50.
- Kichatov, B., Korshunov, A., Sudakov, V. and Golubkov, A., Evaporation of ferrofluid drop in magnetic field in Leidenfrost mode, Journal of Magnetism and Magnetic Materials, Vol.588, (2023), DOI:10.1016/j.jmmm.2023.171410.
- Kim, D.E., Dynamic Leidenfrost temperature behaviors on uniformly distributed micropillars, Experimental Thermal and Fluid Science, Vol.111, (2020), DOI:10.1016/j.expthermflusci.2019.109954.
- Kim, H., Truong, B., Buongiorno, J. and Hu, L.W., On the effect of surface roughness height, wettability, and nanoporosity on Leidenfrost phenomena, Applied Physics Letters, Vol.98, No.8 (2011), DOI:10.1063/1.3560060.
- Kim, S.H., Lee, G., Kim, H. and Kim, M.H., Leidenfrost point and droplet dynamics on heated micropillar array surface, International Journal of Heat and Mass Transfer, Vol.139, (2019), pp.1-9.
- Kim, S.H., Seon Ahn, H., Kim, J., Kaviany, M. and Hwan Kim, M., Dynamics of water droplet on a heated nanotubes surface, Applied Physics Letters, Vol.102, No.23 (2013), DOI:10.1063/1.4809944.
- Kita, Y., Nakamatsu, M., Hidaka, S., Kohno, M. and Takata, Y., Quenching mechanism of spray cooling and the effect of system pressure, International Journal of Heat and Mass Transfer, Vol.190, (2022), DOI:10.1016/j.ijheatmasstransfer.2022.122795.
- Kwon, H.M., Bird, J.C. and Varanasi, K.K., Increasing Leidenfrost point using micro-nano hierarchical surface structures, Applied Physics Letters, Vol.103, No.20 (2013), DOI:10.1063/1.4828673.
- Lee, G.C., Kim, S.H., Kang, J.Y., Kim, M.H. and Jo, H., Leidenfrost temperature on porous wick surfaces: Decoupling the effects of the capillary wicking and thermal properties, International Journal of Heat and Mass Transfer, Vol.145, (2019), DOI:10.1016/j.ijheatmasstransfer.2019.118809.
- Lee, S.H., Lee, S.J., San Lee, J., Fezzaa, K. and Je, J.H., Transient dynamics in drop impact on a superheated surface, Physical Review Fluids, Vol.3, No.12 (2018), DOI:10.1103/PhysRevFluids.3.124308.
- Leidenfrost, J.G., De aquae communis nonnullis qualitatibus tractatus (1756), Ovenius (In German).
- Li, A., Li, H., Lyu, S., Zhao, Z., Xue, L., Li, Z., Li, K., Li, M., Sun, C. and Song, Y., Tailoring vapor film beneath a Leidenfrost drop, Nature Communications, Vol.14, No.1 (2023), DOI:10.1038/s41467-023-38366-z.
- Li, D., Zhu, Z. and Sun, D.W., Effects of freezing on cell structure of fresh cellular food materials: A review, Trends in Food Science & Technology, Vol.75, (2018), pp.46-55.
- Lim, E., Ng, B.T., Hung, Y.M. and Tan, M.K., Graphene-mediated suppression of Leidenfrost effect for droplets on an inclined surface, International Journal of Thermal Sciences, Vol.174, (2022), DOI:10.1016/j.ijthermalsci.2021.107426.
- Lin, K., Chen, S., Zeng, Y., Ho, T.C., Zhu, Y., Wang, X., Liu, F., Huang, B., Chao, C.Y.H., Wang, Z. and Tso, C.Y., Hierarchically structured passive radiative cooling ceramic with high solar reflectivity, Science, Vol.382, No.6671 (2023), pp.691-697.
- Lin, Y., Zhao, C., Chu, F., Wu, X. and Miljkovic, N., Leidenfrost droplet billiard balls, Physical Review Fluids, Vol.9, No.11 (2024), DOI:10.1103/PhysRevFluids.9.L111601.
- Liu, D. and Tran, T., Size-dependent spontaneous oscillations of Leidenfrost droplets, Journal of Fluid Mechanics, Vol.902, (2020), DOI:10.1017/jfm.2020.576.
- Lu, Y., Bao, J. and Liu, D., An experimental and theoretical investigation of electrostatic suppression of the Leidenfrost state, International Journal of Heat and Mass Transfer, Vol.170, (2021), DOI:10.1016/j.ijheatmasstransfer.2021.121036.
- Lyu, S., Tan, H., Wakata, Y., Yang, X., Law, C.K., Lohse, D. and Sun, C., On explosive boiling of a multicomponent Leidenfrost drop, Proceedings of the National Academy of Sciences, Vol.118, No.2 (2021), DOI:10.1073/pnas.2016107118.
- Malenkov, I., Detachment frequency as a function of size for vapor bubbles, Journal of Engineering Physics, Vol.20, No.6 (1971), pp.704-708.
- Maquet, L., Brandenbourger, M., Sobac, B., Biance, A.L., Colinet, P. and Dorbolo, S., Leidenfrost drops: Effect of gravity, Europhysics Letters, Vol.110, No.2 (2015), DOI:10.1209/0295-5075/110/24001.
- Nair, H., Staat, H.J., Tran, T., van Houselt, A., Prosperetti, A., Lohse, D. and Sun, C., The Leidenfrost temperature increase for impacting droplets on carbon-nanofiber surfaces, Soft Matter, Vol.10, No.13 (2014), pp.2102-2109.
- Nazari, H. and Pournaderi, P., The electric field effect on the droplet collision with a heated surface in the Leidenfrost regime, Acta Mechanica, Vol.230, (2019), pp.787-804.

- Ng, B.T., Hung, Y.M. and Tan, M.K., Acoustically-controlled Leidenfrost droplets, Journal of Colloid and Interface Science, Vol.465, (2016), pp.26-32.
- Ng, B.T., Hung, Y.M. and Tan, M.K., Suppression of the Leidenfrost effect via low frequency vibrations, Soft Matter, Vol.11, No.4 (2015), pp.775-784.
- Orejon, D., Sefiane, K. and Takata, Y., Effect of ambient pressure on Leidenfrost temperature, Physical Review E, Vol.90, No.5 (2014), DOI:10.1103/PhysRevE.90.053012.
- Ozkan, O., Shahriari, A. and Bahadur, V., Electrostatic suppression of the Leidenfrost state using AC electric fields, Applied Physics Letters, Vol.111, No.14 (2017), DOI:10.1063/1.4999174.
- Pacheco-Vazquez, F., Ledesma-Alonso, R., Palacio-Rangel, J.L. and Moreau, F., Triple Leidenfrost effect: Preventing coalescence of drops on a hot plate, Physical Review Letters, Vol.127, No.20 (2021), DOI:10.1103/PhysRevLett.127.204501.
- Paul, G., Das, P.K. and Manna, I., Droplet oscillation and pattern formation during Leidenfrost phenomenon, Experimental Thermal and Fluid Science, Vol.60, (2015), pp.346-353.
- Paul, G., Das, P.K. and Manna, I., Nanoparticle deposition from nanofluid droplets during Leidenfrost phenomenon and consequent rise in transition temperature, International Journal of Heat and Mass Transfer, Vol.148, (2020), DOI:10.1016/j.ijheatmasstransfer.2019.119110.
- Piroird, K., Texier, B.D., Clanet, C. and Quéré, D., Reshaping and capturing Leidenfrost drops with a magnet, Physics of Fluids, Vol.25, No.3 (2013), DOI:10.1063/1.4796133.
- Prasad, D., Sharma, A. and Dash, S., Influence of the substrate permeability on Leidenfrost temperature, International Journal of Heat and Mass Transfer, Vol.178, (2021), 10.1016/j.ijheatmasstransfer.2021.121629.
- Prasad, G.V.V., Dhar, P. and Samanta, D., Postponement of dynamic Leidenfrost phenomenon during droplet impact of surfactant solutions, International Journal of Heat and Mass Transfer, Vol.189, (2022), DOI:10.1016/j.ijheatmasstransfer.2022.122675.
- Qiao, Y. and Chandra, S., Boiling of droplets on a hot surface in low gravity, International Journal of Heat and Mass Transfer, Vol.39, No.7 (1996), pp.1379-1393.
- Quéré, D., Leidenfrost dynamics, Annual Review of Fluid Mechanics, Vol.45, (2013), pp.197-215.
- Rasheed, R.M., Thomas, E.A., Gardner, P., Rogers, T., Verduzco, R. and Weislogel, M.M., Omni-gravity nanophotonic heating and leidenfrost-driven water recovery system, Gravitational and Space Research, Vol.8, No.1 (2020), pp.31-44.
- Sahoo, V., Lo, C.W. and Lu, M.C., Leidenfrost suppression and contact time reduction of a drop impacting on silicon nanowire array-coated surfaces, International Journal of Heat and Mass Transfer, Vol.148, (2020), DOI:10.1016/j.ijheatmasstransfer.2019.118980.
- Sajadi, S.M., Irajizad, P., Kashyap, V., Farokhnia, N. and Ghasemi, H., Surfaces for high heat dissipation with no Leidenfrost limit, Applied Physics Letters, Vol.111, No.2 (2017), DOI:10.1063/1.4993775.
- Sen, S., Vaikuntanathan, V. and Sivakumar, D., Impact dynamics of alternative jet fuel drops on heated stainless steel surface, International Journal of Thermal Sciences, Vol.121, (2017), pp.99-110.
- Sen, U., Roy, T., Ganguly, R., Angeloni, L.A., Schroeder, W.A. and Megaridis, C.M., Explosive behavior during binary-droplet impact on superheated substrates, International Journal of Heat and Mass Transfer, Vol.154, (2020), DOI: 10.1016/j.ijheatmasstransfer.2020.119658.
- Shahriari, A., Ozkan, O. and Bahadur, V., Electrostatic suppression of the Leidenfrost state on liquid substrates, Langmuir, Vol.33, No.46 (2017), pp.13207-13213.
- Shahriari, A., Wurz, J. and Bahadur, V., Heat transfer enhancement accompanying Leidenfrost state suppression at ultrahigh temperatures, Langmuir, Vol.30, No.40 (2014), pp.12074-12081.
- Shirota, M., van Limbeek, M.A., Sun, C., Prosperetti, A. and Lohse, D., Dynamic Leidenfrost effect: Relevant time and length scales, Physical Review Letters, Vol.116, No.6 (2016), DOI:10.1103/PhysRevLett.116.064501.
- Situ, W., Zambrano, H.A. and Walther, J.H., Water nanofilm boiling on a copper surface in the presence of dissolved air, Applied Thermal Engineering, Vol.244, (2024), DOI:10.1016/j.applthermaleng.2024.122697.
- Snoeijer, J.H., Brunet, P. and Eggers, J., Maximum size of drops levitated by an air cushion, Physical Review E, Vol.79, No.3 (2009), DOI:10.1103/PhysRevE.79.036307.
- Sobac, B., Rednikov, A., Dorbolo, S. and Colinet, P., Self-propelled Leidenfrost drops on a thermal gradient: A theoretical study, Physics of Fluids, Vol.29, No.8 (2017), DOI:10.1063/1.4990840.

- Sun, X.Z., Li, Q., Li, W.X., Wen, Z.X. and Liu, B., Enhanced pool boiling on microstructured surfaces with spatially-controlled mixed wettability, International Journal of Heat and Mass Transfer, Vol.183, (2022), DOI:10.1016/j.ijheatmasstransfer.2021.122164.
- Talari, V., Behar, P., Lu, Y., Haryadi, E. and Liu, D., Leidenfrost drops on micro/nanostructured surfaces, Frontiers in Energy, Vol.12, (2018), pp.22-42.
- Tamvada, S., Attinger, D. and Moghaddam, S., On critical heat flux and its evaporation momentum and hydrodynamic limits, International Journal of Heat and Mass Transfer, Vol.203, (2023), DOI:10.1016/j.ijheatmasstransfer.2022.123837.
- Tominaga, T., Hachiya, M., Tatsuzaki, H. and Akashi, M., The accident at the Fukushima Daiichi nuclear power plant in 2011, Health Physics, Vol.106, No.6 (2014), pp.630-637.
- Tran, T., Staat, H.J., Susarrey-Arce, A., Foertsch, T.C., van Houselt, A., Gardeniers, H.J., Prosperetti, A., Lohse, D. and Sun, C., Droplet impact on superheated micro-structured surfaces, Soft Matter, Vol.9, No.12 (2013), pp.3272-3282.
- Ulahannan, L., Krishnakumar, K., Nair, A.R. and Ranjith, S.K., An experimental study on the effect of nanoparticle shape on the dynamics of Leidenfrost droplet impingement, Experimental and Computational Multiphase Flow, Vol.3, (2021), pp.47-58.
- Utaka, Y., Kashiwabara, Y. and Ozaki, M., Microlayer structure in nucleate boiling of water and ethanol at atmospheric pressure, International Journal of Heat and Mass Transfer, Vol.57, No.1 (2013), pp.222-230.
- Van Erp, R., Soleimanzadeh, R., Nela, L., Kampitsis, G. and Matioli, E., Co-designing electronics with microfluidics for more sustainable cooling, Nature, Vol.585, No.7824 (2020), pp.211-216.
- Van Limbeek, M.A.J., Ramirez-Soto, O., Prosperetti, A. and Lohse, D., How ambient conditions affect the Leidenfrost temperature, Soft Matter, Vol.17, No.11 (2021), pp.3207-3215.
- Vara Prasad, G., Sharma, H., Nirmalkar, N., Dhar, P. and Samanta, D., Augmenting the Leidenfrost temperature of droplets via nanobubble dispersion, Langmuir, Vol.38, No.51 (2022), pp.15925-15936.
- Villegas, L.R., Tanguy, S., Castanet, G., Caballina, O. and Lemoine, F., Direct numerical simulation of the impact of a droplet onto a hot surface above the Leidenfrost temperature, International Journal of Heat and Mass Transfer, Vol.104, (2017), pp.1090-1109.
- Wakata, Y., Zhu, N., Chen, X., Lyu, S., Lohse, D., Chao, X. and Sun, C., How roughness and thermal properties of a solid substrate determine the Leidenfrost temperature: Experiments and a model, Physical Review Fluids, Vol.8, No.6 (2023), DOI:10.1103/PhysRevFluids.8.L061601.
- Wang, G., Fei, L., Lei, T., Wang, Q. and Luo, K.H., Droplet impact on a heated porous plate above the Leidenfrost temperature: A lattice Boltzmann study, Physics of Fluids, Vol.34, No.9 (2022), DOI:10.1063/5.0118079.
- Wang, L., Li, X., Wang, Z., Tian, H., Wang, C., Chen, X. and Shao, J., Suppressing the Leidenfrost effect by air discharge assisted electrowetting-on-dielectrics, Applied Physics Letters, Vol.125, No.2 (2024), DOI:10.1063/5.0206395.
- Wyatt, B.C., Nemani, S.K., Hilmas, G.E., Opila, E.J. and Anasori, B., Ultra-high temperature ceramics for extreme environments, Nature Reviews Materials, Vol.9, No.773-789 (2023), DOI:10.1038/s41578-023-00619-0.
- Yang, J., Li, Y., Fan, Y., Chen, L., Wang, D. and Deng, X., A standing Leidenfrost drop with sufi-whirling, Proceedings of the National Academy of Sciences, Vol.120, No.32 (2022), DOI:10.1073/pnas.2305567120.
- Yim, E., Bouillant, A., Quéré, D. and Gallaire, F., Leidenfrost flows: Instabilities and symmetry breakings, Flow, Vol.2, (2022), DOI:10.1017/flo.2022.5.
- Zhai, L., Yang, K., Jin, K., Liang, Y. and Liu, C., CFD-aided method for evaporation modelling and heat transfer optimization of high-temperature surfaces considering Leidenfrost effects, International Communications in Heat and Mass Transfer, Vol.158, (2024), DOI:10.1016/j.icheatmasstransfer.2024.107904.
- Zhang, L., Gong, S., Lu, Z., Cheng, P. and Wang, E.N., Boiling crisis due to bubble interactions, International Journal of Heat and Mass Transfer, Vol.182, (2022), DOI:10.1016/j.ijheatmasstransfer.2021.121904.
- Zhang, P., Peng, B., Yang, X., Wang, J. and Jiang, L., Regulating droplet dynamic wetting behaviors using surfactant additives on high-temperature surfaces, Advanced Material Interfaces, Vol.7, No.14 (2020), DOI:10.1002/admi.202000501.
- Zhao, T.Y. and Patankar, N.A., The thermo-wetting instability driving Leidenfrost film collapse, Proceedings of the National Academy of Sciences, Vol.117, No.24 (2020), pp.13321-13328.